EC/GCI SALTeXPERT WORKSHOP, November 2002, Prague
www.itam.cas.cz/~arcchip/

THE DAMAGE MECHANISM OF SODIUM SULFATE IN POROUS STONE

E. Doehne[1], C. Selwitz[2], and D. Carson[1]

[1]The Getty Conservation Institute, 1200 Getty Center Drive, Suite 700, Los Angeles, CA 90049, USA, TEL: (310) 440 6237, FAX: 310 440 7711, Email: edoehne@getty.edu, [2]3631 Surfwood road, Malibu, CA, 90265, USA.

1. Summary

Why is sodium sulfate so damaging to porous building materials? This question has remained unanswered for at least 170 years, since sodium sulfate began to be used to test the relative durability of different stones (de Thury 1828; Luquer 1895). Two important areas of recent research on this topic are 1) the non-equilibrium crystallization of thenardite (Na_2SO_4) and 2) the generation of high supersaturation ratios and rapid mirabilite ($Na_2SO_4 \cdot 10H_2O$) crystallization by placing a saturated solution of sodium sulfate in contact with fine-grained thenardite crystals.

Two sets of experiments were performed to test the role of these processes: 1) macro experiments of "rising damp" crystallization of sodium sulfate in limestone blocks under conditions of high and low air exchange rate. In an attempt to determine the phase causing the important initial damage, spall fragments resulting from the high air exchange rate samples were studied by ESEM for crystal type, morphology and distribution of salt adjacent to conchoidal fractures in the calcite substrate. 2) Dynamic ESEM crystallization experiments with sodium sulfate solutions undertaken to examine the hypothesis that dissolution of thenardite in a sodium sulfate solution should be followed by rapid mirabilite precipitation.

Some authors have suggested that the decay of stone from sodium sulfate occurs primarily through the crystallization of mirabilite from a supersaturated solution. Based on our "rising damp" experiments of contour scaling dynamics, this does not appear to be the case where high air exchange leads to a concentration of damage just below the surface. Instead, the non-equilibrium crystallization of small thenardite crystals appears to be responsible for the damage.

Dynamic ESEM experiments with sodium sulfate confirm the rapid precipitation of euhedral mirabilite after dissolution of fine-grained thenardite in a sodium sulfate solution. This suggests that the damage caused in the standardized laboratory salt crystallization test is due to a different damage mechanism than is typically observed in decay of stone in the field.

2. Introduction

The crystallization of soluble salts in porous building materials is a widespread weathering process that results in damage to important architecture, monuments and archaeological sites (Arnold & Zehnder 1991; Goudie & Viles 1997). Salt weathering by thenardite (Na_2SO_4) and mirabilite ($Na_2SO_4 \cdot 10H_2O$) is especially destructive, yet is still not fully understood (Price 1978; Charola & Weber 1992; McMahon, Sandberg *et al.* 1992; Doehne 1994; Grossi, Esbert *et al.* 1997; Rodriguez-Navarro, Doehne *et al.* 2000).

The complexity of the salt weathering system can be reduced by focusing on the moment, type and extent of damage that takes place (Fig. 1). There appear to be three general kinetic pathways that result in enhanced damage due to salt crystallization: 1) rapid drying, 2) rapid cooling (for salts with a variation in solubility with temperature), and 3) contact between saturated salt solutions and pre-existing fine-grained salts, especially in the case of thenardite. Previous work has shown that airflow (drying rate) also appears to have a significant role in salt weathering (Doehne & Rodríguez-Navarro 1996; Rodriguez-Navarro, Doehne *et al.* 1999).

Flatt (2002b) has recently proposed that an important decay pathway for sodium sulfate is the dissolution of thenardite in a saturated sodium sulfate solution, resulting in damage from the rapid growth of mirabilite. This decay path is what is expected in the standard RILEM (1980) and ASTM (1997) salt crystallization tests. Here we present new experimental data that further addresses these questions, helps explain why sodium sulfate is so damaging and also shows how changes in airflow can substantially reduce salt damage in laboratory experiments.

3. Testing Building Materials with Sodium Sulfate

The standard salt crystallization tests (ASTM and RILEM) for building materials, where sample blocks are repeatedly immersed in saturated solutions of sodium sulfate and then dried, are widely used to estimate resistance to frost damage and relative durability of stones (Price 1978; Marschner 1979). Price (1978) found that the degree of damage caused by the sodium sulfate crystallization test was "…strongly dependant upon solution concentration, solution temperature and rate of drying." There has been some controversy over the applicability of the tests, given the severity of the test and the sometimes inconsistent results (Sheftick 1989; Hunt 1994). Recent research has addressed this problem from two directions: examining the way the test actually operates (Rodriguez-Navarro, Doehne *et al.* 2000) and proposing new standard test methods which more closely simulate typical conditions (Benavente, Ordóñez *et al.* 2001). The assumption of many researchers has been that the damage from this test occurred due to the hydration of sodium sulfate. More recent work suggests that direct crystallization of thenardite may occur at lower RH conditions during drying (Rodriguez-Navarro, Doehne *et al.* 2000) in addition to rapid mirabilite crystallization during wetting (Doehne, Selwitz *et al.* 2001; Flatt 2002b). Goudie (1999) found that salt crystallization tests of limestone were poor predictors of frost resistance. Efforts to discover parameters that correlate with relative building stone durability continue, with emphasis on those that can be measured more easily than salt crystallization resistance (Moh'd, Howarth *et al.* 1996; Ordonez, Fort *et al.* 1997; Nicholson 2001).

4. Materials and Methods

For the first set of "rising damp" experiments, a capillarity setup (Fig. 2) similar to that described by Rodríguez-Navarro and Doehne (1999b) was used. Typically, a tared 800 ml crystallization dish was placed on a balance and the salt, water, limestone column, and wax were added and weighed sequentially. In each experiment, enough water was added to provide 400 g of sodium sulfate solution (5, 15 and 20% concentration). All the concentrations are given on a weight basis. Solution flow rates and general efflorescence/subflorescence behavior for these experiments has been reported separately (Selwitz & Doehne 2002). Bath limestone was used for experiments based on its known vulnerability to salt decay and abundant fine pores (Fig. 3). The 3 x 3 x 25 cm stone column of limestone was placed to stand upright in the center of the dish. Molten household paraffin wax was added to hold the column and seal the system so that water is lost only by passage up through the column. The starting weight of the setup was taken just after the wax was poured. When the components in the experiment were in place, the arrangement was either put on a bench in a well-ventilated laboratory maintained at a relative humidity of ~43% or placed in a large draft-free plastic box that was not hermetically sealed (high humidity, low airflow). The solution wicks up through the limestone column and water is lost by evaporation from the surfaces. Depending on the storage conditions and exposure time, varying patterns of salt emergence and stone damage occur. Draftiness in the laboratory can effect flow-through rates in the capillarity setups (Selwitz & Doehne 2002). The studies to examine high airflow conditions were done in a well-ventilated room that had an air exchange rate that varied between 6 and 12 changes per hour (average of 10). Samples were documented with still photography before and after the evaporation of the salt solution (about 3 weeks in the case of the high airflow samples). One experiment (20%, high air flow) was also documented using time-lapse video according to the method described previously (Rodriguez-Navarro & Doehne 1999b).

From the deteriorated stone surface of the high airflow setup, spall samples that were about to fall were removed to maintain orientation and ensure observation of the inner surface where the break was propagated. The samples examined at 1 Torr water vapor pressure in a field emission Environmental SEM (FEI XL30 ESEM FEG)(Doehne 1997). These conditions prevent hydration of thenardite and would cause a slow, observable dehydration of mirabilite into a "fluffy" matrix that would pseudomorphically resemble the original mirabilite crystals (Doehne 1994; Rodriguez-Navarro, Doehne *et al.* 2000). In combination with ESEM/EDS analysis, this preparation method allows the identification of the type of crystal present on the limestone spall surfaces. Samples that were found to contain only thenardite were then lightly coated with Pd to reduce beam penetration to better resolve crystals on the 30-500 nm scale.

In the second set of experiments, the behavior of sodium sulfate was documented in the Environmental SEM (ESEM) using saturated solutions of sodium sulfate both alone and in contact with small fragments of Bath limestone. A peltier stage was used in the ESEM to cool the salt solutions to 2°C. The ESEM imaging conditions used were 20 KeV with a water vapor concentration varying from 2-5 Torr. The relative humidity in the ESEM was cycled in order to move through the sodium sulfate stability field from solution, to mirabilite crystallization, and then to dehydration of thenardite (Fig. 4 & 5). Then water was condensed on the thenardite matrix to simulate re-wetting of stone. Rapid mirabilite crystallization was generally observed after this re-wetting of the fine thenardite crystals.

5. Results

Observations of contour scaling dynamics in the first set of experiments show that damage appears to be an episodic process based on transient stress and loss of surface material (repeated millimeter-scale spalling) under conditions of high air flow (Fig. 6-8). Control and low airflow samples show a different pattern (Fig. 9 & 10). For the high air flow samples showing extensive damage, the sudden initial fracture of a surface spall or scale is often followed by a more gradual lifting of the flake over several days by further pushing by salt growth until the spall falls off (Fig. 11-14). Inner spall surfaces are characterized by concentrations of anhedral microcrystalline thenardite (Fig. 15-17), with the size of the salt crystals increasing somewhat with distance from the stone surface (Fig. 23 & 24). Image analysis of spall surfaces by ESEM consistently finds very small crystals (<1 µm) of thenardite (Na_2SO_4) adjacent to conchoidal fractures in the calcite matrix (Fig. 16). Bladed, type III thenardite (Rodriguez-Navarro, Doehne *et al.* 2000) is observed in some areas (Fig. 21 & 22), but appears to be less common adjacent to fracture surfaces than fine anhedral thenardite. The "bacterial" appearance of the thenardite crystals is consistent with their being precipitated rapidly at high supersaturation ratios (Sunagawa 1981). It should be clear that the thenardite crystals observed on the spall fragment surfaces have not resulted from the dehydration of mirabilite crystals, based on their morphology (compact, not "fluffy") and lack of pseudomorphic appearance. Examples of the characteristic dehydrated appearance of thenardite derived from mirabilite can be seen in Rodriguez-Navarro, Doehne and others (2000).

The geometry of the crystallization and stone surface loss appears to be controlled by the environmental conditions of the experiments (~43% RH and 10 air exchanges per hour). The high airflow supports crystallization under the surface of the stone, compared to substantial efflorescence for the samples under conditions of low air exchange rate. This work provides additional confirmation of the drying rate as a key parameter in salt weathering, as well as suggesting that changing the location of crystallization by modifying the drying rate may help reduce damage from sodium sulfate. The fact that thenardite is the crystal form observed, rather than the expected mirabilite suggests that greater consideration needs to be paid to the non-equilibrium behavior of salts in order to better understand and mitigate damage. Mirabilite does not readily crystallize in the absence of a seed crystal (Arnold, personal communication). This behavior typically leads to either high supersaturations before mirabilite crystallization occurs, or the direct crystallization of thenardite. The important step of oven-drying samples as part of the standard sodium sulfate crystallization test ensures the elimination of any potential mirabilite seed crystals.

Dynamic ESEM experiments with sodium sulfate confirm the rapid precipitation of euhedral mirabilite after dissolution of fine-grained thenardite in a sodium sulfate solution (Fig. 25 & 26). Digital video of these dynamic experiments is available from the authors. The results suggest that the presence of a pre-existing fine-grained salt matrix is an important element in explaining the severe damage resulting from the standard ASTM and RILEM salt crystallization tests (Fig. 27). Results from dynamic ESEM experiments also show that rapid hydration of thenardite may occur in the absence of liquid water when the crystal size is small (<10 µm). The rate of hydration may be related in part to the lower pressure in the ESEM. More rapid drying kinetics than typically seen at atmospheric pressure have been observed in drying leather in the ESEM (Tuckermann, Mertig *et al.* 2001). Humidity-controlled XRD of the thenardite/mirabilite transition has been explored by Steiger and others (2000b), and show that the hydration of mirabilite from thenardite in the absence of liquid water appears to take place as a gradual transition.

Why is sodium sulfate so damaging to porous materials? Results from laboratory crystallization experiments in stone with sodium sulfate provide information that confirms the importance of the direct precipitation of thenardite in contour scaling damage to limestone. The rapid crystallization of mirabilite after dissolution of thenardite is also confirmed in ESEM experiments. The direct precipitation of thenardite below 32.4 °C may cause more damage than mirabilite crystallization, since using the Correns (1949) equation it has been determined that thenardite has a much higher crystallization pressure at the same supersaturation ratio (Winkler & Singer 1972). The fact that the vast majority of thenardite crystals on the calcite spall surface appear to be well-adhered suggests that the dissolution of calcite under pressure and the embedding of thenardite may have taken place during the transient stress of confined crystal growth. It may be possible to section these crystals to determine the attachment geometry in future work.

6. Discussion

Sodium sulfate is widely recognized as one of the most damaging salts to porous materials. The sodium sulfate system consists of sodium sulfate decahydrate – mirabilite ($Na_2SO_4 \cdot 10H_20$) and sodium sulfate (anhydrous) — or thenardite (Na_2SO_4). Previous theoretical and experimental work suggests a number of ways damage can occur, including crystallization and hydration. Hydration has been observed to take place through dissolution and reprecipitation, and can be considered a special case of crystallization (Doehne 1994; Flatt 2002a).

Salt damage theory suggests that the limiting factor in causing damage is the need to sustain a solution *in situ* with a high supersaturation ratio (Rodriguez-Navarro & Doehne 1999a). This is generally difficult in many porous materials since their naturally rough surfaces tend to enhance crystallization once saturation is reached. Several authors have asked the question: how do you maintain such a high supersaturation ratio for a solution in a porous material with abundant nucleation sites? (C. Price in Goudie & Viles 1997; Doehne 2002). NaCl for example, has been observed to readily crystallize and not reach high supersaturation ratios before crystallizing in porous materials (Rodriguez-Navarro & Doehne 1999a; Hees & Lubelli 2002).

In addition to rapid drying, rapid cooling is also an important way to obtain a high supersaturation ratio in the sodium sulfate system (Figs. 4, 5, 27). Our *in situ* observations suggest that the process of cyclic dehydration followed by contact with a saturated solution of sodium sulfate can also result in rapid crystal growth and potential damage to porous materials.

While equilibrium thermodynamics is essential tool in understanding salt crystallization (Price 2000; Scherer 2000; Steiger, Beyer *et al.* 2000a), we argue here based on accumulated field observations and laboratory experiments that in some circumstances salt weathering appears to be a non-equilibrium process that involves the rapid growth of small confined crystals in fine pores (often poorly formed), resulting in transient tensile stress and crack propagation. Kinetic factors appear to play a critical role in the generation of conditions that result in damage. Large, well-formed crystals associated with salt weathering may typically occur after the initial damage, during recrystallization and extrusion of efflorescence (Arnold & Zehnder 1991; Scherer 2002). It is hoped that the results discussed in this work will help aid in the understanding of these complex processes so that a better model of how they actually take place on the nanometer to millimeter scale can be developed. A more complete picture of the decay mechanism is clearly a useful step in the development of more effective damage mitigation strategies.

Mitigation methods such as limiting the rapid cooling or rapid drying of porous, salt-laden stone through the use of shelters and removal of existing salts were possible should reduce the damage potential of sodium sulfate. Wetting a stone containing abundant, fine-grained thenardite in order to desalinate it should be done with care, since if the solution becomes concentrated in some microporous areas due to incomplete wetting, crystallization of mirabilite and damage may result.

7. Conclusions

The experiments performed here show that draft-free, high humidity environments enhance efflorescence and substantially reduce damage. This is consistent with a model of salt decay that assumes that the location of crystallization and the supersaturation ratio reached can be manipulated to reduce damage. Experimental evidence further supports the non-equilibrium crystallization of thenardite (Na_2SO_4) as a major cause of damage. The postulated rapid precipitation of euhedral mirabilite after dissolution of fine-grained thenardite in a sodium sulfate solution is also confirmed by dynamic ESEM experiments with sodium sulfate. This suggests that the damage caused in the standardized laboratory salt crystallization test (mirabilite crystallization) is due to a different damage mechanism than is typically observed in decay of stone in the field (thenardite crystallization).

References

Arnold, A. & Zehnder, K., 1991. Monitoring wall paintings affected by soluble salts, The Conservation of Wall Paintings. Proceedings of a symposium organized by the Courtauld Institute of Art and the Getty Conservation Institute, London, July 13-16, 1987. Getty Conservation Institute, Marina del Rey, pp. 103-135.

ASTM, 1997. ASTM C88-90, Standard test method for soundness of aggregate by use of sodium sulfate or magnesium sulfate, Annual Book of ASTM Standards 4.2. ASTM, pp. 37-42.

Benavente, D., Ordóñez, S. *et al.*, 2001. Quantification of salt weathering in porous stones using an experimental continuous partial immersion method. *Engineering geology*, **59**(3-4): 313-325.

Charola, A.E. & Weber, J., 1992. The hydration-dehydration mechanism of sodium sulphate. In: J.D. Rodrigues, F. Henriques and F.T. Jeremisas (Editors), 7th International Congress on Deterioration and Conservation of Stone, Lisbon Portugal, 15-18 June 1992, Proceedings. Laboratorio Nacional de Engenharia Civil, Lisbon, Portugal, pp. 581-590.

Correns, C.W., 1949. Growth and dissolution of crystals under linear pressure. *Discussions of the Faraday Society, London*, **5**: 267-271.

de Thury, H., 1828. Sur le procede propose par M. Brard pour reconnaitre immediatement les pierres qui ne peuvent pas resister a la gelee, et que l'on designe ordinairement par les noms de pierres gelives ou pierres gelisses = On the method proposed by Mr. Brard for the immediate detection of stones unable to resist the action of frost. *Annales de chimie et de physique*, **38**: 160-192.

Doehne, E., 1994. In situ dynamics of sodium sulfate hydration and dehydration in stone pores: Observations at high magnification using the environmental scanning electron microscope. In: V. Fassina, H. Ott and F. Zezza (Editors), The conservation of monuments in the Mediterranean Basin. Proceedings of the 3rd International Symposium, Venice, 1994 (La conservazione dei monumenti nel bacino del Mediterraneo Atti del 3o Simposio Internazionale, Venezia, 1994). Soprintendenza ai Beni Artistici e Storici di Venezia, pp. 143-150.

Doehne, E., 1997. ESEM development and application in cultural heritage conservation. In: P.L. Gai (Editor), In-Situ Microscopy in Materials Research: Leading International Research in Electron and Scanning Probe Microscopies. Kluwer Academic Publishers, pp. 45-62.

Doehne, E., 2002. Salt Weathering: A Selective Review. In: T.W.a.A.V. S. Siegesmund (Editor), Natural Stone, Weathering Phenomena, Conservation Strategies and Case Studies. The Geological Society of London, Special Publication 205.

Doehne, E. & Rodríguez-Navarro, C., 1996. Salt damage: New insights from time-lapse experiments, Geological Society of America, Program with Abstracts, 1. Geological Society of America, Denver, pp. 51252.

Doehne, E., Selwitz, C. *et al.*, 2001. Damage to monuments from the crystallization of mirabilite, thenardite and halite: mechanisms, environment, and preventive possibilities, Eleventh Annual V. M. Goldschmidt Conference. Geochemical Society, pp. 3212.pdf.

Flatt, R.J., 2002a. Hydration Pressure: A bad case of crystallization pressure, SALTeXPERT Workshop. GCI/ARIADNE, Prague, http://www.itam.cas.cz/~arcchip/.

Flatt, R.J., 2002b. Salt damage in porous materials: how high supersaturations are generated. *Journal of crystal growth*, **242**(3-4): 435-454.

Goudie, A.S., 1999. A comparison of the relative resistance of limestones to frost and salt weathering. *Permafrost and Periglacial Processes*, **10**(4): 309-316.

Goudie, A.S. & Viles, H., 1997. Salt Weathering Hazards. John Wiley, Chichester, 241 pp.

Grossi, C.M., Esbert, R.M. *et al.*, 1997. Acoustic emission monitoring to study sodium sulphate crystallization in monumental porous carbonate stones. *Stud. Conserv.*, **42**: 115-25.

Hees, R.v. & Lubelli, B., 2002. Analysis of transport and crystallization of salts in restoration plasters, SALTeXPERT Workshop. GCI/ARIADNE, Prague, http://www.itam.cas.cz/~arcchip/.

Hunt, B., 1994. There's no alternative. *Stone industries*, **February**: 5,8,37-39.

Luquer, L.M., 1895. The relative effects of frost and sulphates of soda efflorescence tests on building stones. *American Society of Civil Engineers - Transactions*, **33**: 235-247 and 247-256.

Marschner, H., 1979. Application of salt crystallisation test to impregnated stones. *Researchs in Archaeology and Conservation*: 70-77.

McMahon, D.J., Sandberg, P. *et al.*, 1992. Deterioration mechanisms of sodium sulfate. In: J.D. Rodrigues, F. Henriques and F.T. Jeremisas (Editors), 7th International Congress on Deterioration and Conservation of Stone, Lisbon Portugal, 15-18 June 1992, Proceedings. Laboratorio Nacional de Engenharia Civil, Lisbon, Portugal, pp. 705-714.

Moh'd, B.K., Howarth, R.J. *et al.*, 1996. Rapid prediction of Building Research Establishment limestone durability class from porosity and saturation. *Quarterly Journal of Engineering Geology*, **29**(4): 285-297.

Nicholson, D.T., 2001. Pore properties as indicators of breakdown mechanisms in experimentally weathered limestones. *Earth Surface Processes and Landforms*, **26**(8): 819-838.

Ordonez, S., Fort, R. *et al.*, 1997. Pore size distribution and the durability of a porous limestone. *Quarterly Journal of Engineering Geology*, **30**(3): 221-230.

Price, C., 2000. Salt Damage in Porous Materials. In: C. Price (Editor), An expert chemical model for determining the environmental conditions needed to prevent salt damage in porous materials, University College London.

Price, C.A., 1978. The use of sodium sulphate crystallisation test for determining the weathering resistance of untreated stone, Alteration et protection des monuments en pierre : colloque international : Paris, du 5 au 9 juin 1978 = Deterioration and protection of stone monuments : International Symposium : Paris, June 5th-9th 1978. Unesco-Rilem, Paris, pp. 10 7??

RILEM, 1980. Recommandations provisoires / Tentative Recommendations. (RILEM) Commission 25-PEM. Protection et erosion des monuments: Essais recommandés pour mesurer l'altération des pierres et évaluer l'efficacité des méthodes de traitement. *Matériaux et Constructions*, **13**(75): 175-253.

Rodriguez-Navarro, C. & Doehne, E., 1999a. Salt weathering: influence of evaporation rate, supersaturation and crystallization pattern. *Earth Surface Processes and Landforms*, **24**(3): 191-209.

Rodriguez-Navarro, C. & Doehne, E., 1999b. Time-lapse video and ESEM: Integrated tools for understanding processes in situ. *American Laboratory*(May): 28-35.

Rodriguez-Navarro, C., Doehne, E. *et al.*, 1999. Origins of honeycomb weathering: The role of salts and wind. *Bulletin of The Geological Society of America*, **111**(8): 1250-1255.

Rodriguez-Navarro, C., Doehne, E. *et al.*, 2000. How does sodium sulfate crystallize? Implications for the decay and testing of building materials. *Cement and concrete research*, **30**(10): 1527-1534.

Scherer, G.W., 2000. Stress from crystallization of salt in pores. In: V. Fassina (Editor), 9th International Congress on Deterioration and Conservation of Stone. Elsevier, Amsterdam, Venice, 19-24 June, pp. 187-194.

Scherer, G.W., 2002. Factors affecting crystallization pressure, RILEM meeting on Delayed Ettringite Formation. RILEM, Villars.

Selwitz, C. & Doehne, E., 2002. The evaluation of crystallization modifiers for controlling salt damage to limestone. *Journal of Cultural Heritage*, **3**(3): 205-216.

Sheftick, 1989. Na2SO4 Soundness Test Evaluation. *Cement, concrete and aggregates*, **11**(1): 73-79.

Steiger, M., Beyer, R. *et al*., 2000a. A thermodynamic model of the Na+–Ca2+–Cl––CH3COO––H2O system. In: C.A. Price (Editor), An expert chemical model for determining the environmental conditions needed to prevent salt damage in porous materials. ECOS: Environmental Control of Salts. European Commission Research Report 11, Protection and Conservation of European Cultural Heritage. Archetype Publications, London, pp. 45-52.

Steiger, M., Beyer, R. *et al*., 2000b. Data Compilation and Experimental Determinations. In: C.A. Price (Editor), An expert chemical model for determining the environmental conditions needed to prevent salt damage in porous materials. ECOS: Environmental Control of Salts. European Commission Research Report 11, Protection and Conservation of European Cultural Heritage. Archetype Publications, London, pp. 19-37.

Sunagawa, I., 1981. Characteristics of crystal growth in nature as seen from the morphology of mineral crystals. *Bulletin Minéralogie*, **104**: 81-87.

Tuckermann, M., Mertig, M. *et al*., 2001. In situ observation of moisture-induced swelling of leather in an environmental scanning electron microscope. *Review of Scientific Instruments*, **72**(2): 1449.

Winkler, E. & Singer, P., 1972. Crystallization pressure of salts in stone and concrete. *Geological Society of America Bulletin*, **83**(11): 3509-3513.

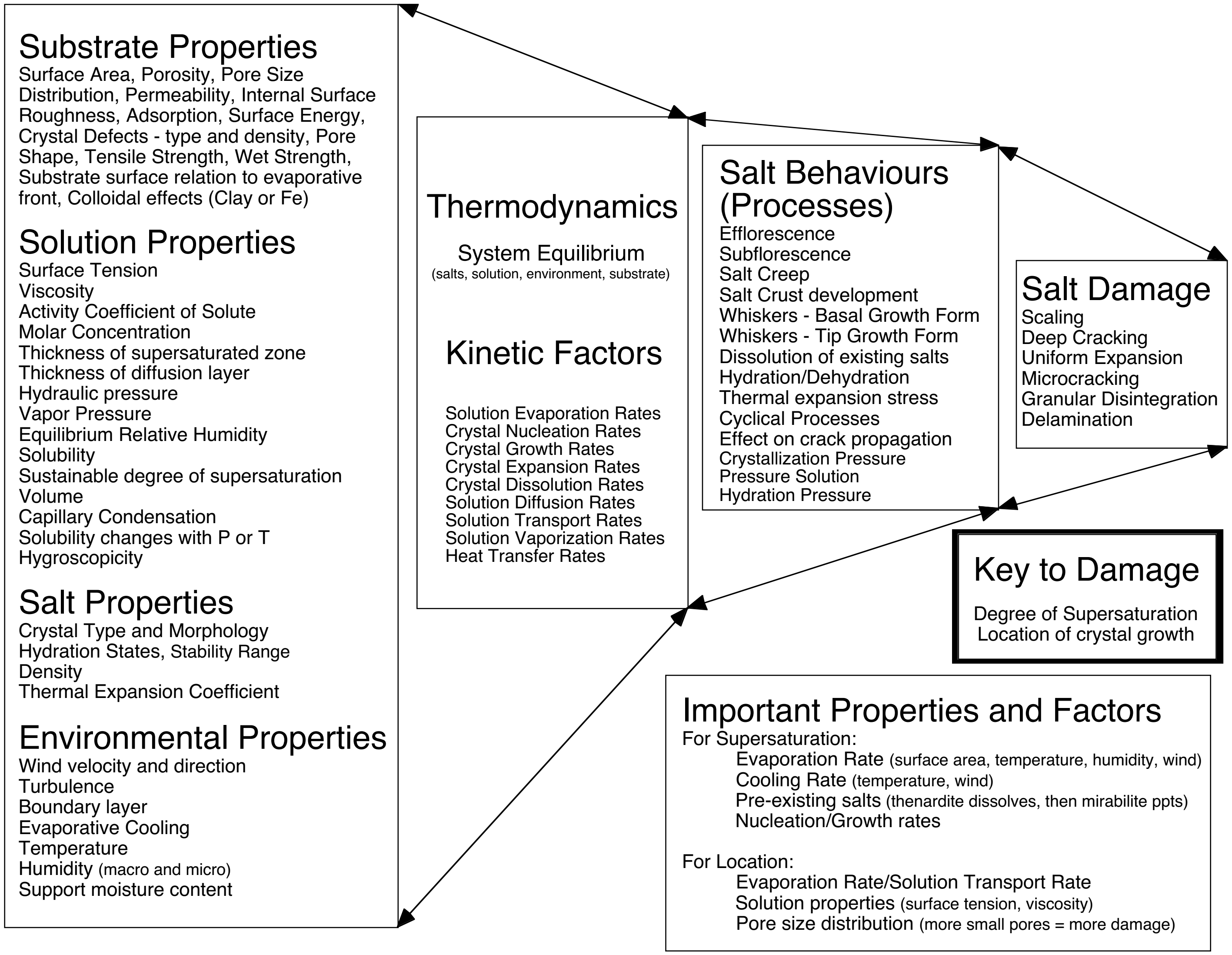

Figure 1. Diagram of properties, factors and behaviours in the salt crystallization process.

Substrate Properties

Surface Area, Porosity, Pore Size Distribution, Permeability, Internal Surface Roughness, Adsorption, Surface Energy, Crystal Defects - type and density, Pore Shape, Tensile Strength, Wet Strength, Substrate surface relation to evaporative front, Colloidal effects (Clay or Fe)

Solution Properties

Surface Tension
Viscosity
Activity Coefficient of Solute
Molar Concentration
Thickness of supersaturated zone
Thickness of diffusion layer
Hydraulic pressure
Vapor Pressure
Equilibrium Relative Humidity
Solubility
Sustainable degree of supersaturation
Volume
Capillary Condensation
Solubility changes with P or T
Hygroscopicity

Salt Properties

Crystal Type and Morphology
Hydration States, Stability Range
Density
Thermal Expansion Coefficient

Environmental Properties

Wind velocity and direction
Turbulence
Boundary layer
Evaporative Cooling
Temperature
Humidity (macro and micro)
Support moisture content

Thermodynamics

System Equilibrium
(salts, solution, environment, substrate)

Kinetic Factors

Solution Evaporation Rates
Crystal Nucleation Rates
Crystal Growth Rates
Crystal Expansion Rates
Crystal Dissolution Rates
Solution Diffusion Rates
Solution Transport Rates
Solution Vaporization Rates
Heat Transfer Rates

Salt Behaviours (Processes)

Efflorescence
Subflorescence
Salt Creep
Salt Crust development
Whiskers - Basal Growth Form
Whiskers - Tip Growth Form
Dissolution of existing salts
Hydration/Dehydration
Thermal expansion stress
Cyclical Processes
Effect on crack propagation
Crystallization Pressure
Pressure Solution
Hydration Pressure

Salt Damage

Scaling
Deep Cracking
Uniform Expansion
Microcracking
Granular Disintegration
Delamination

Key to Damage

Degree of Supersaturation
Location of crystal growth

Important Properties and Factors

For Supersaturation:
- Evaporation Rate (surface area, temperature, humidity, wind)
- Cooling Rate (temperature, wind)
- Pre-existing salts (thenardite dissolves, then mirabilite ppts)
- Nucleation/Growth rates

For Location:
- Evaporation Rate/Solution Transport Rate
- Solution properties (surface tension, viscosity)
- Pore size distribution (more small pores = more damage)

Figure 2. Experimental Setup for Crystallization Experiments

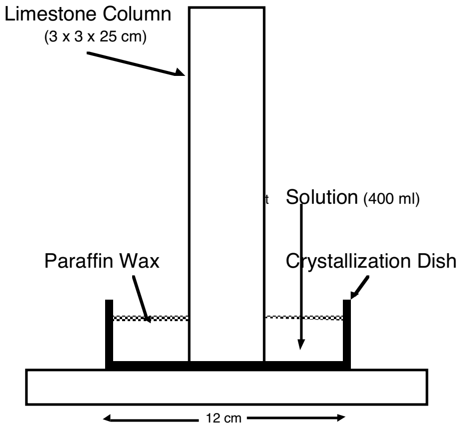

(Humidity is constant and fluid flows upward from base of stone)

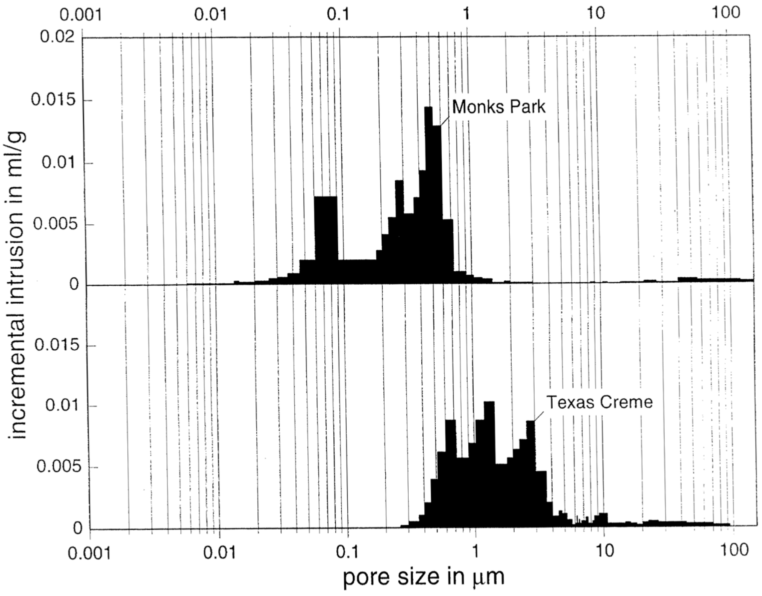

Figure 3. Pore size distribution of Monks Park oolitic limestone and Texas Crème limestone. Note abundance of micropores in the Monks Park stone.

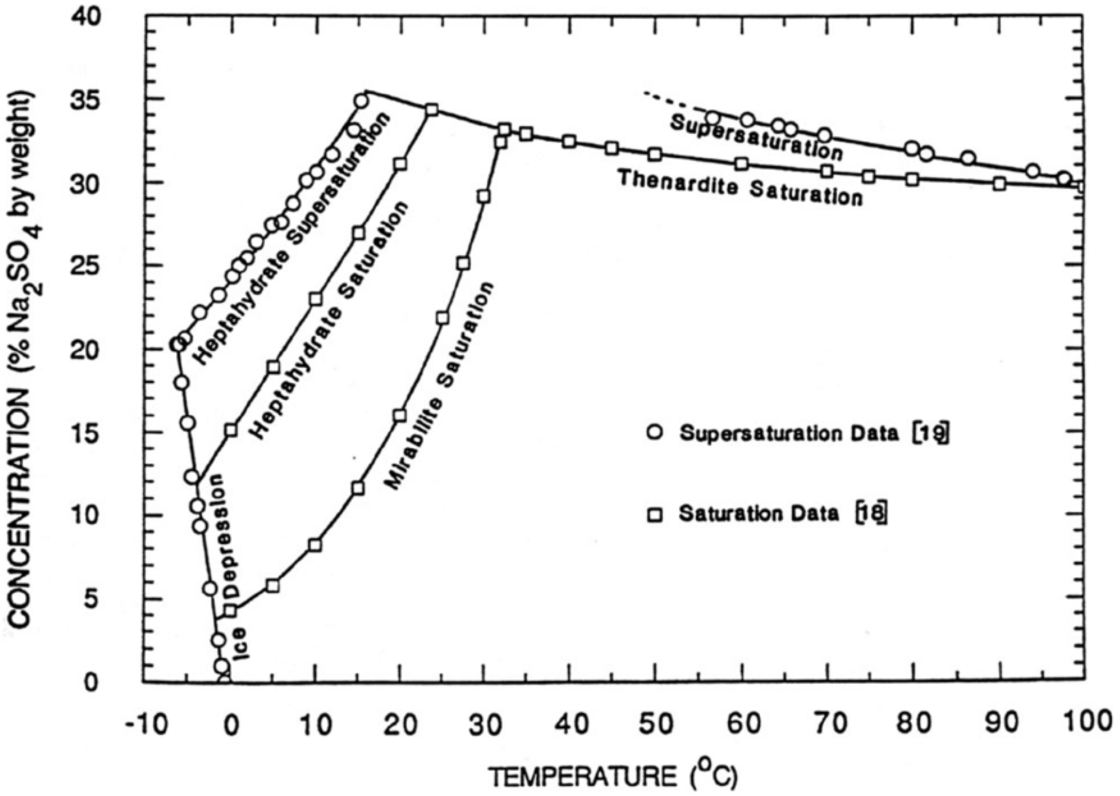

Figure 4. Stability diagram (concentration vs. temperature) for the sodium sulfate system. Saturation and supersaturation curves for the sodium sulfate-water system, including thenardite (Na_2SO_4), mirabilite ($Na_2SO_4•10H_2O$), and metastable heptahydrate ($Na_2SO_4•7H_2O$). Diagram from McMahon (1992), data from Gmelin. Note solubility dependance on temperature of mirabilite.

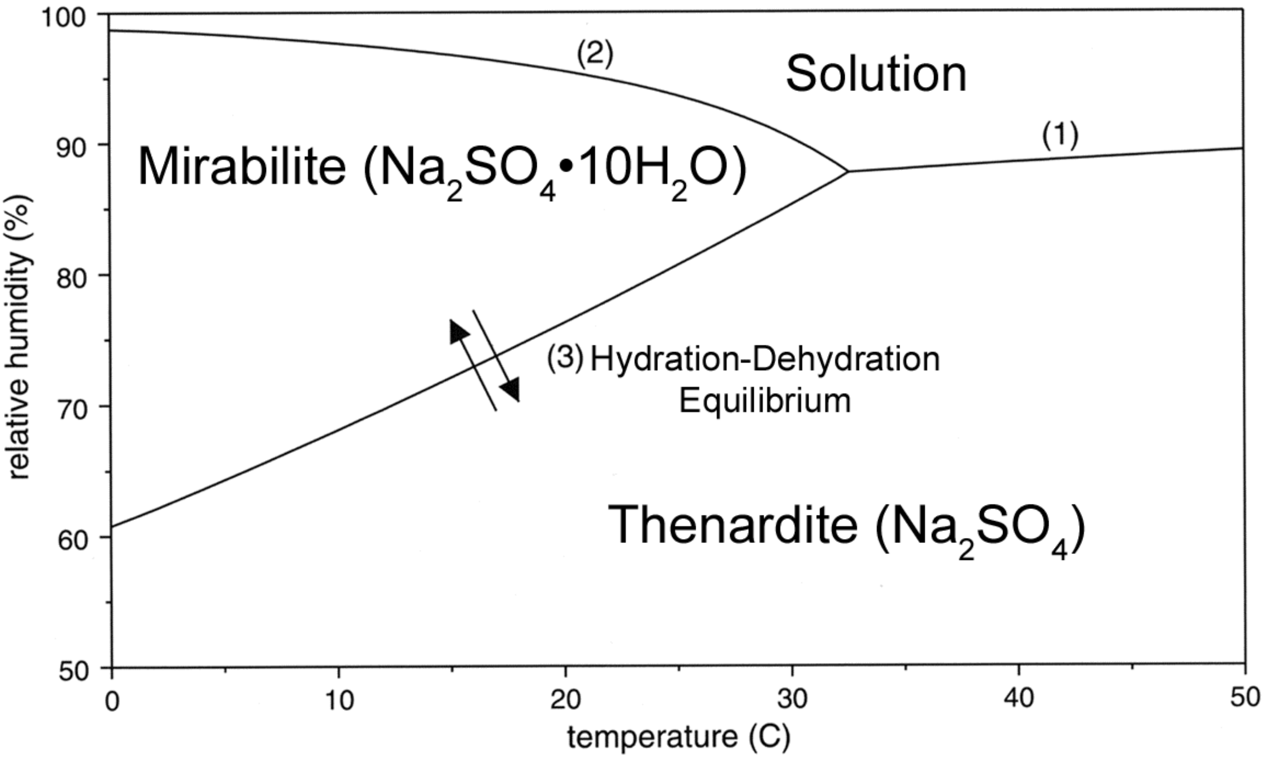

Figure 5. Stability diagram (RH vs. temperature) for the sodium sulfate system. Note strong temperature and RH stability dependance for mirabilite. Crystallization of thenardite is expected below line 1; crystallization of mirabilite is expected below line 2. Note thenardite is not expected to precipitate below ~32.4°C. Mirabilite is expected to dehydrate to thenardite below line 3.

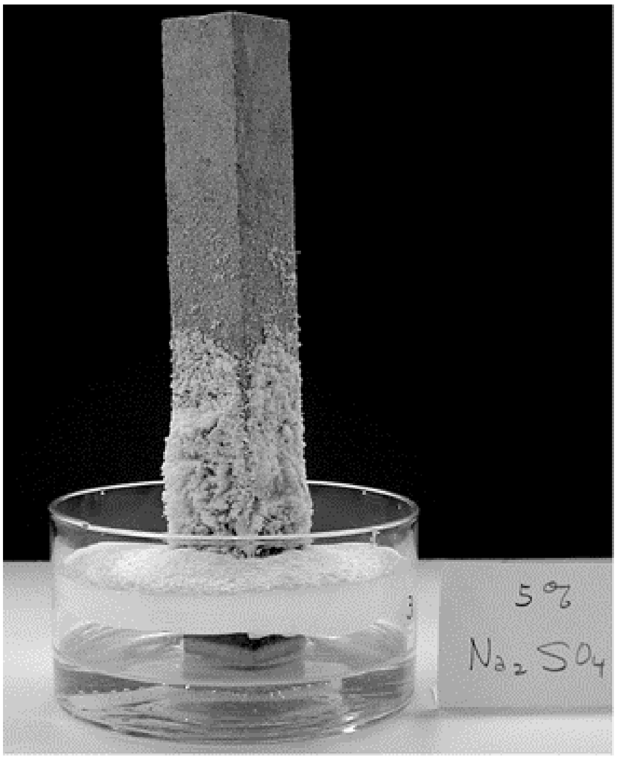

Figure 6. Bath limestone block after exposure to 5% solution of sodium sulfate in high air exchange environment (10x/hr) for two weeks. Note substantial efflorescence.

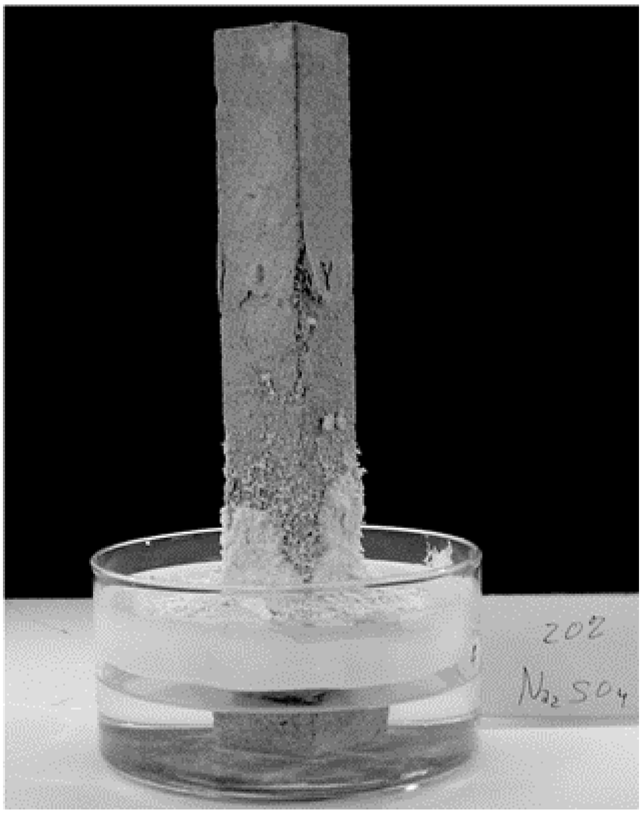

Figure 7. Bath limestone block after exposure to 20% solution of sodium sulfate in high air exchange environment (10x/hr) for two weeks. Note less efflorescence and greater damage due to subsurface crystallization.

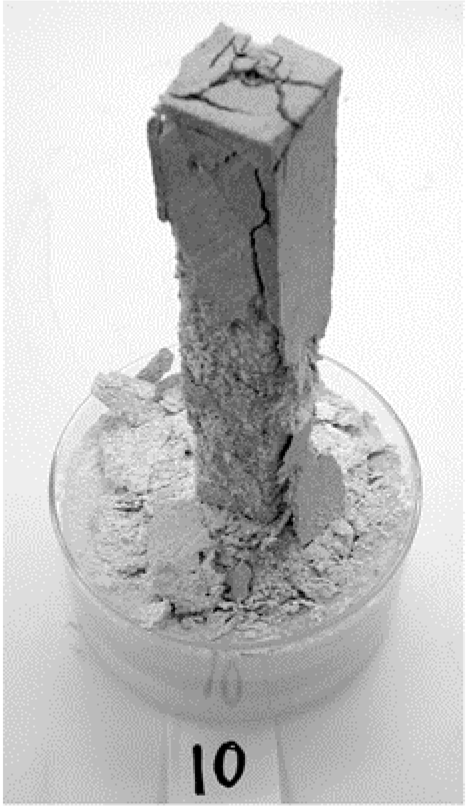

Figure 8. Bath limestone block after exposure to 15% solution of sodium sulfate in high air exchange environment (10x/hr) for four weeks. Note extensive contour scaling.

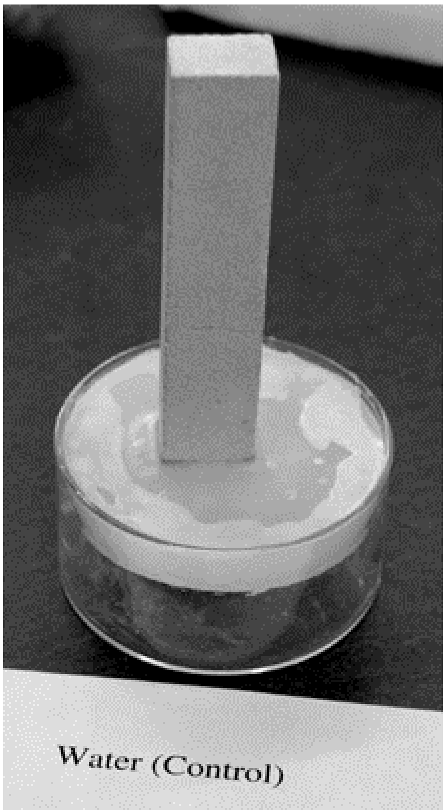

Figure 9. Bath limestone block exposed to water (control). Note no loss of stone surface.

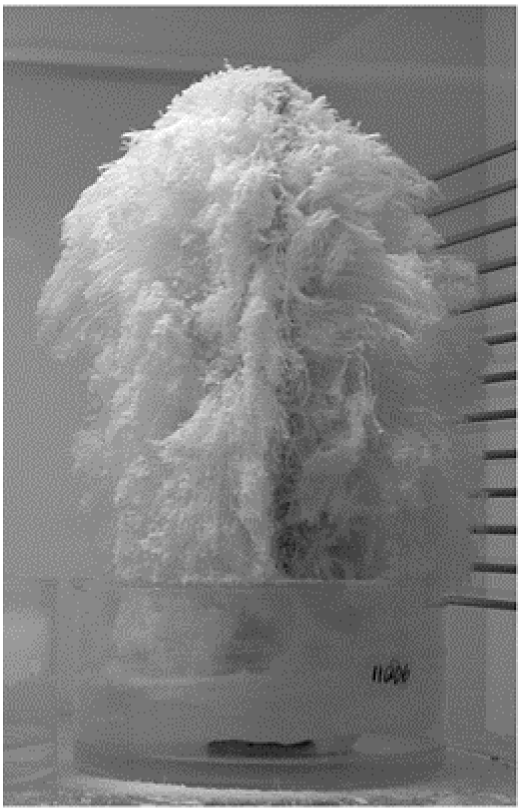

Figure 10. Bath limestone block after exposure to 20% solution of sodium sulfate in low air exchange environment, 3 months. Note extensive efflorescence of mirabilite.

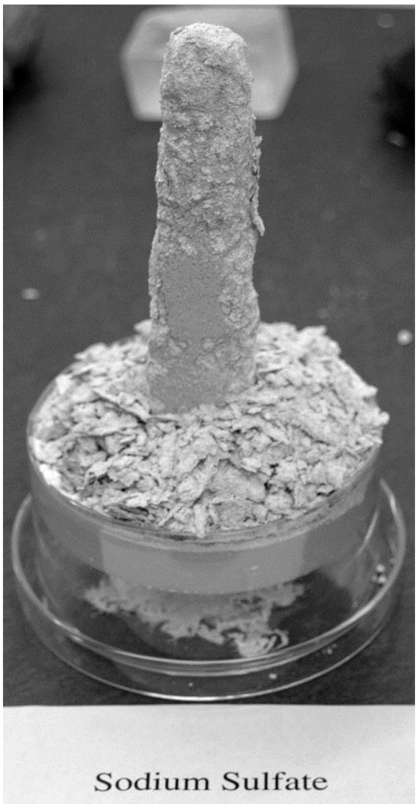

Figure 11. Bath limestone after exposure to 20% solution of sodium sulfate in high air exchange environment (10x/hr), 3 months. Note contour scaling. Note scales at base.

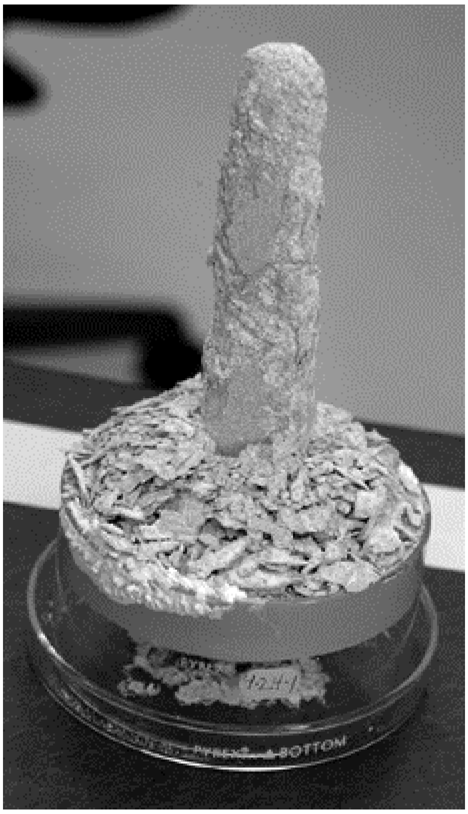

Figure 12. Opposite side of Bath limestone block after exposure to 20% solution of sodium sulfate in high air exchange environment (10x/hr). Note pile of scales at base of sample.

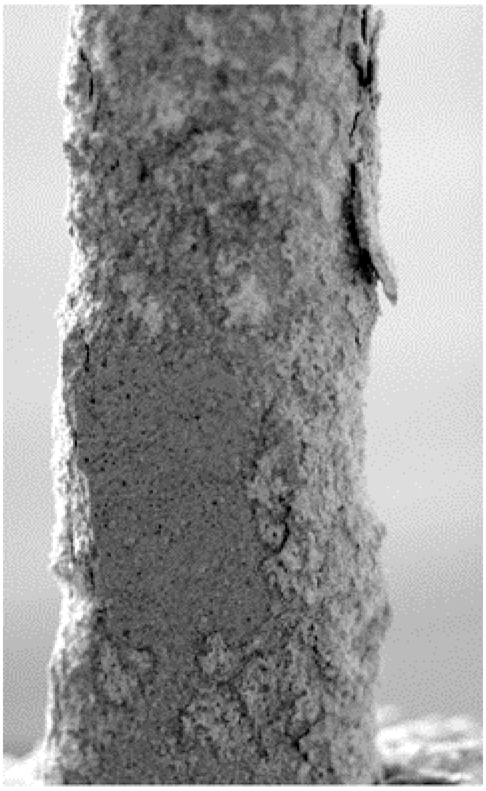

Figure 13. Surface detail of Bath limestone block after exposure to 20% solution of sodium sulfate. Note partially attached contour scales (spall fragments).

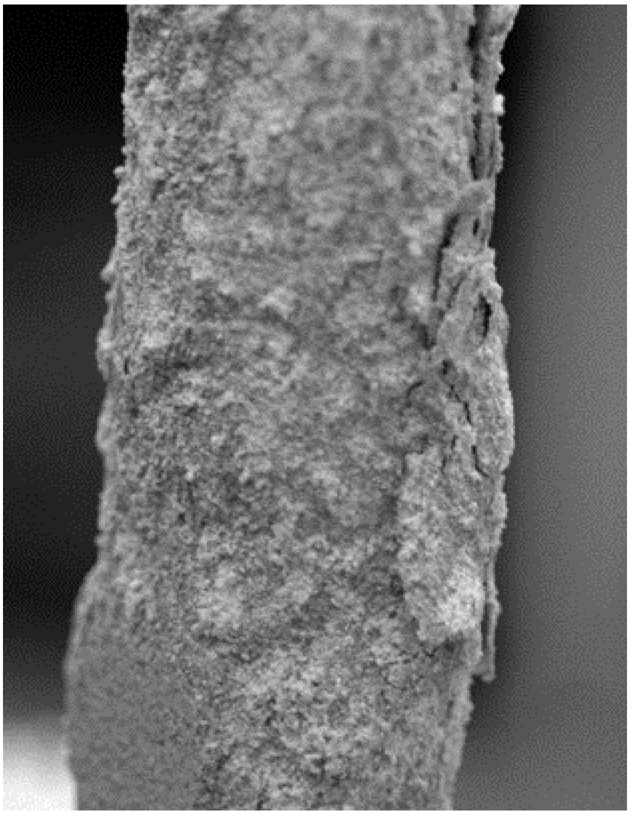

Figure 14. Additional surface detail of Bath limestone block after exposure to 20% solution of sodium sulfate. Note partially attached scales (spall fragments), white salt on surfaces.

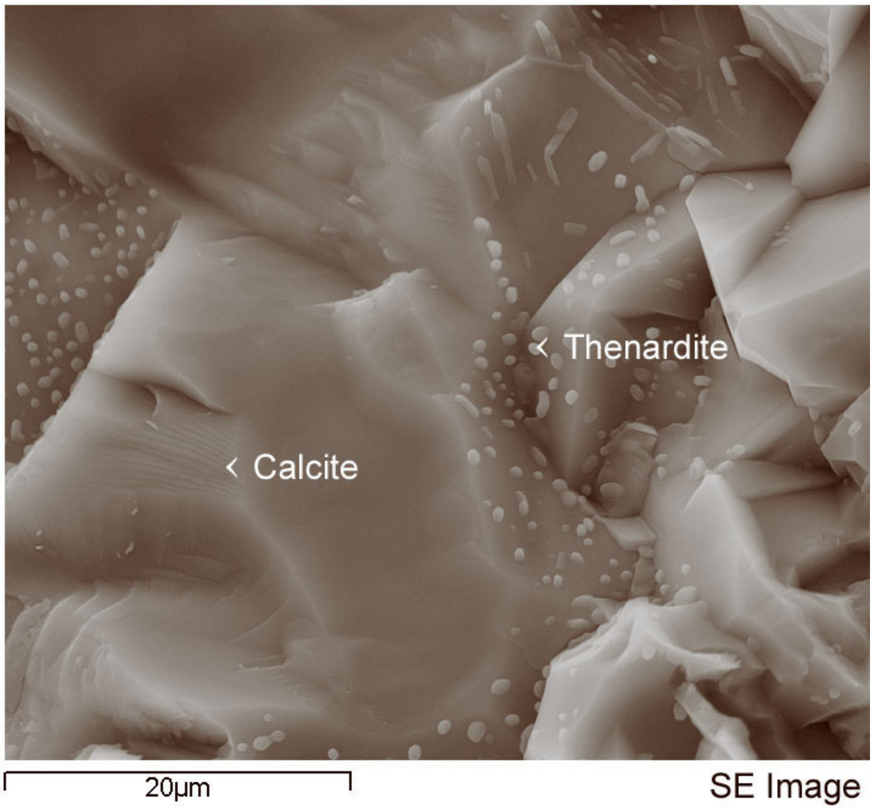

Figure 15. Electron micrograph of inner surface of millimeter-thick scale of Bath limestone (spall fragment). Note large fracture through calcite microspar cement and adjacent micron-scale anhedral thenardite crystals.

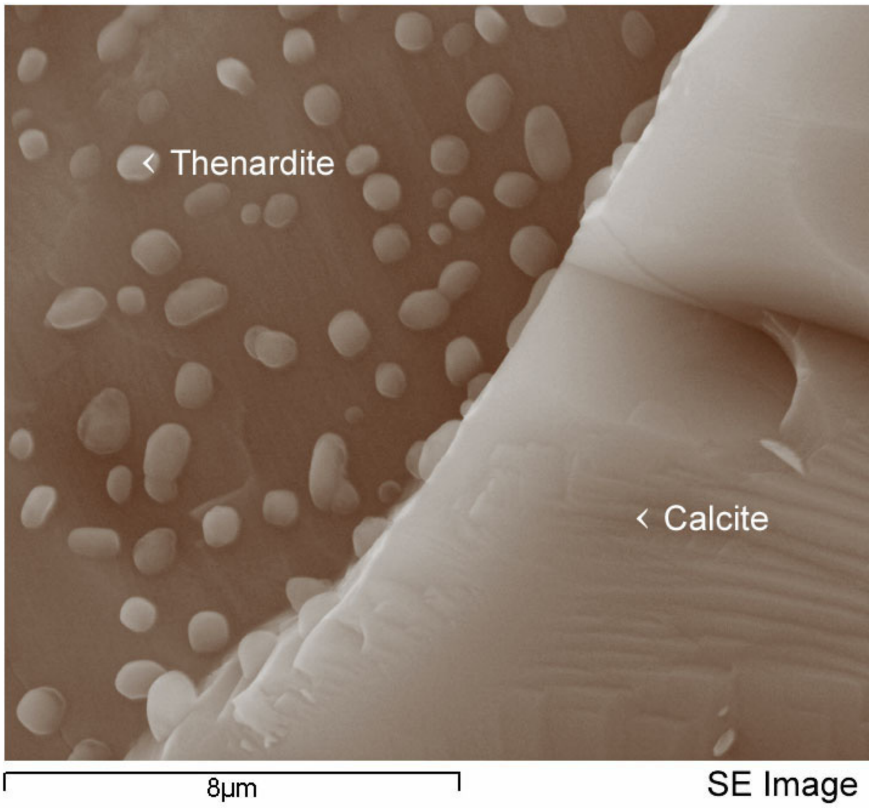

Figure 16. Close-up of inner surface of millimeter-thick scale (spall fragment). Note conchoidal fracture features in calcite and adjacent anhedral thenardite crystals.

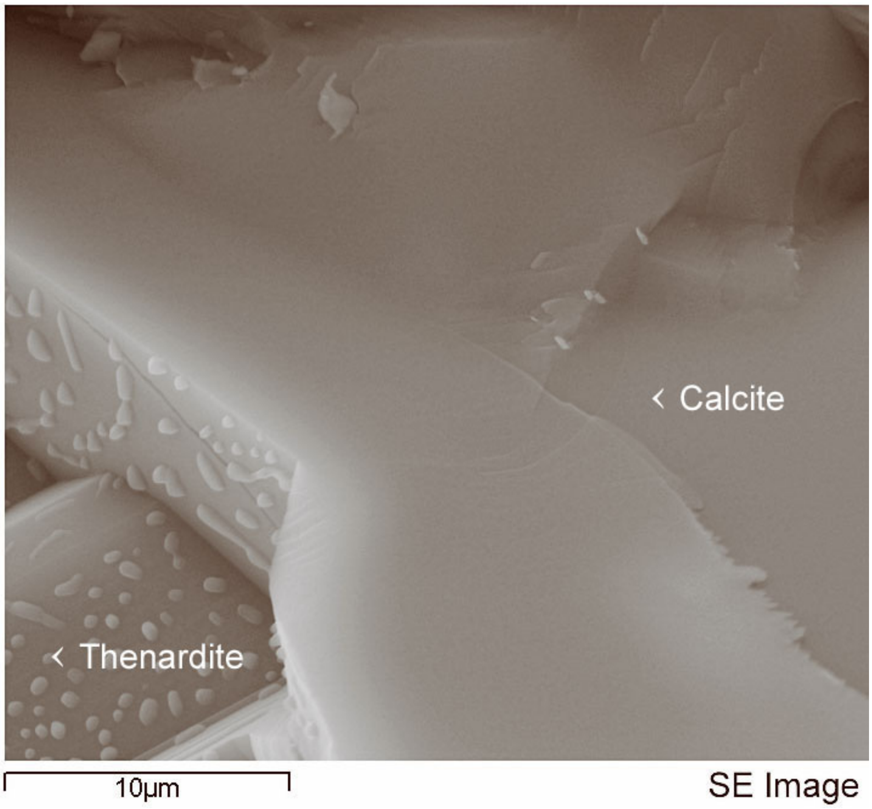

Figure 17. Electron micrograph of inner surface of millimeter-thick scale. Another example of fracture through calcite. Note adjacent thenardite apparently on planar crystal boundary pore space.

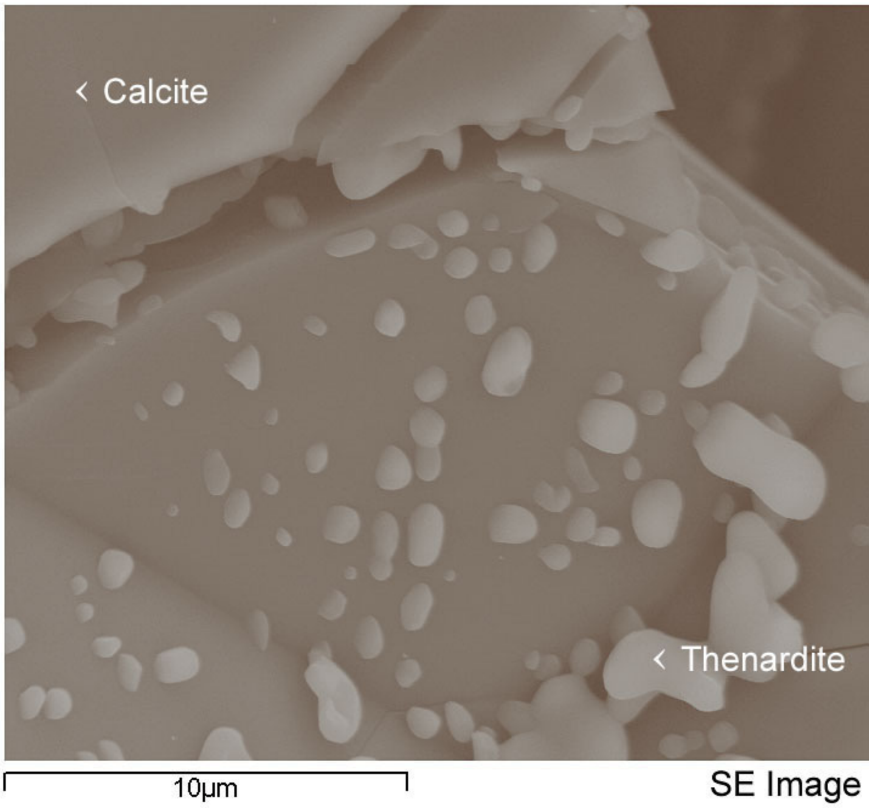

Figure 18. Fracture in calcite with adjacent thenardite. Note thenardite in fracture at top of image.

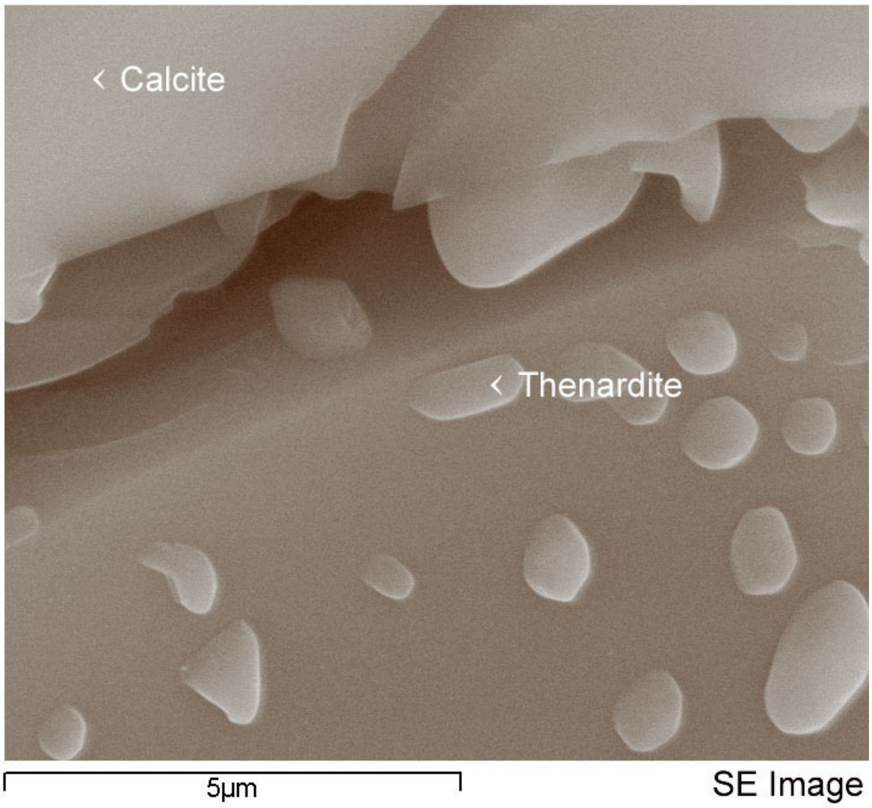

Figure 19. Close-up of thenardite crystals in and adjacent to fracture in calcite microspar. Note anhedral shape of thenardite crystals.

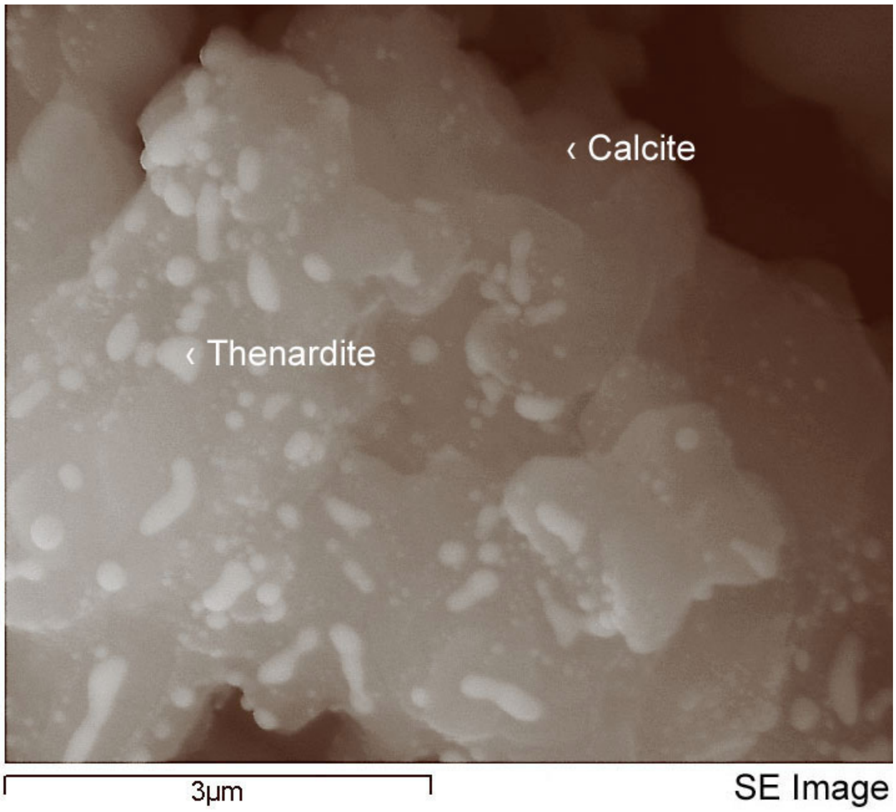

Figure 20. High magnification secondary electron micrograph of surface of scale (spall fragment). Note size distribution of thenardite crystals on calcite surface appears to range from 30 nm to 500 nm. Smallest features in field of view are about 30 nm in size.

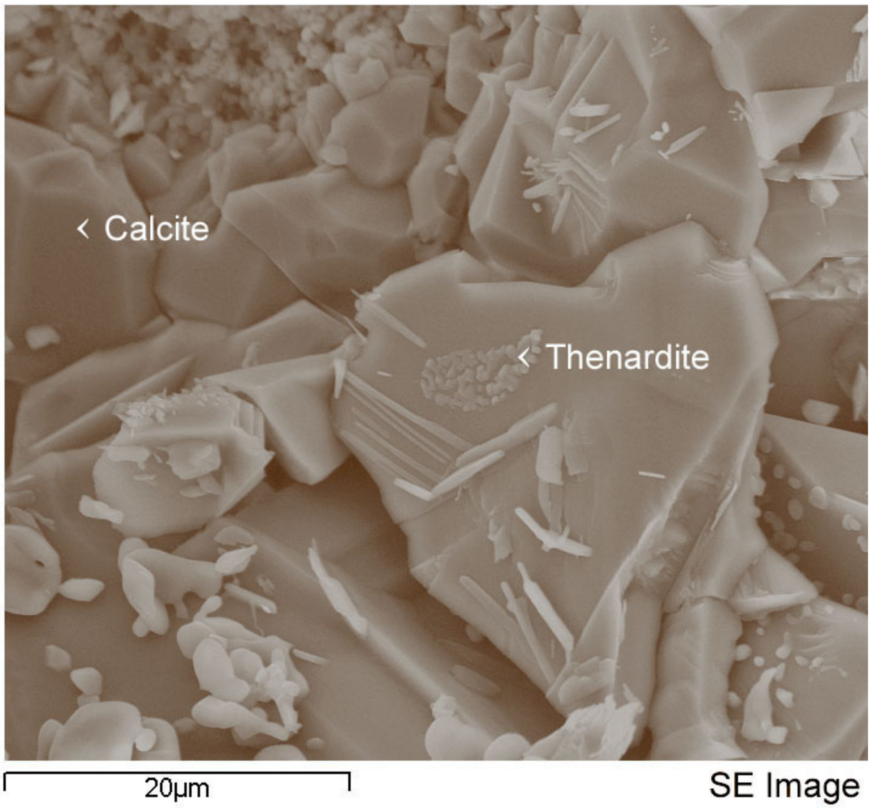

Figure 21. Lower magnification electron micrograph of fracture surface in microsparitic area of Bath limestone scale (spall fragment). Note sodium sulfate in three sizes: submicron (center); type III bladed crystals (see below); and larger 5-10 µm crystals (lower left).

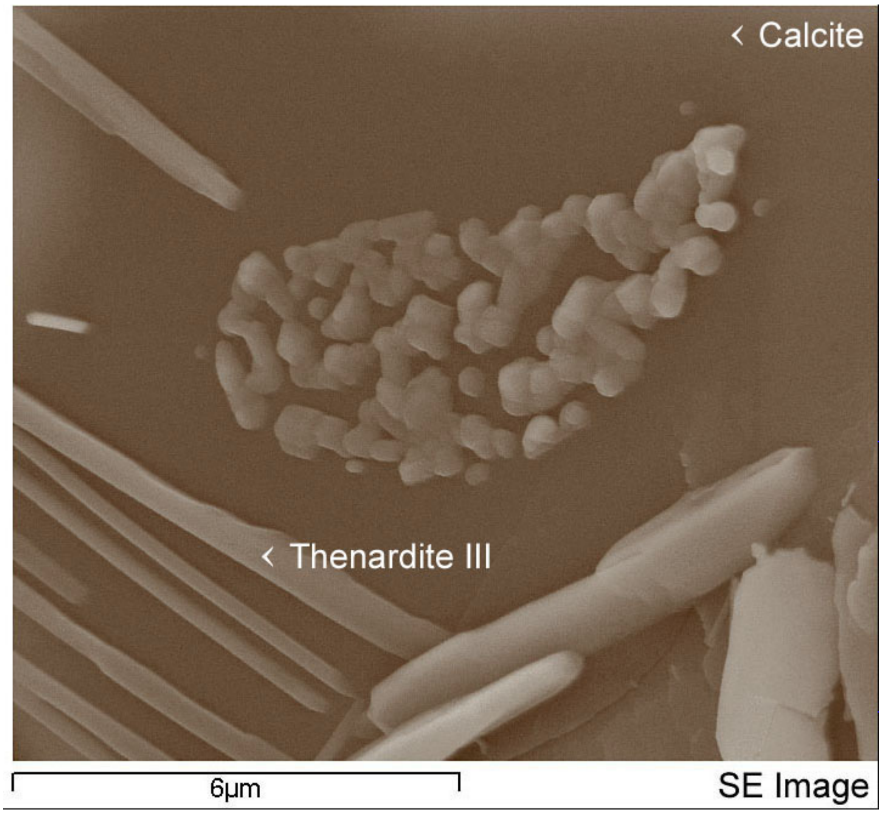

Figure 22. Close-up of above area showing type III bladed crystals of thenardite as well as anhedral submicron forms.

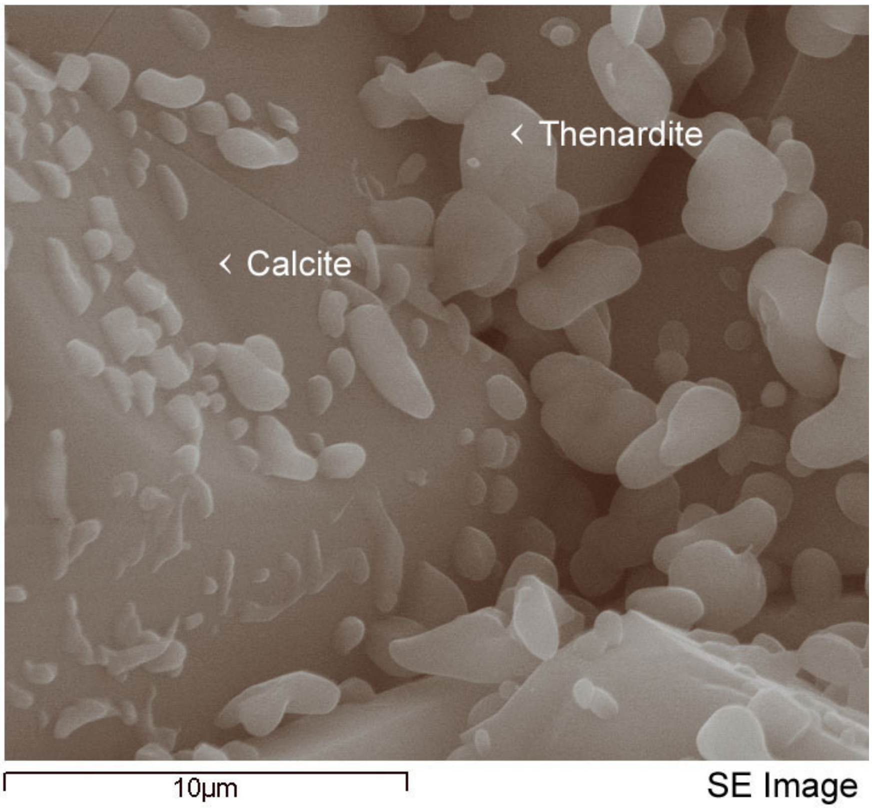

Figure 23. Electron micrograph of "transition area" showing change from submicron thenardite (left) with larger thenardite further away from fracture surface. Hypothesis is that larger crystals grew after smaller crystals and represent lifting of surface after initial damage.

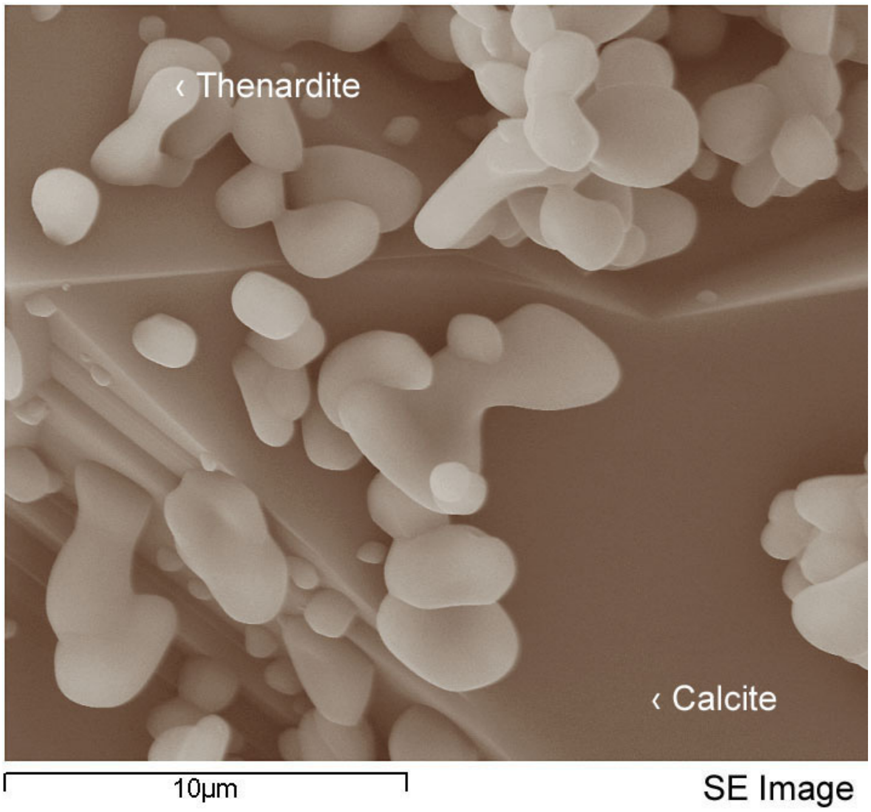

Figure 24. Electron micrograph of larger, anhedral thenarditecrystals on calcite substrate located one millimeter from the fracture area.

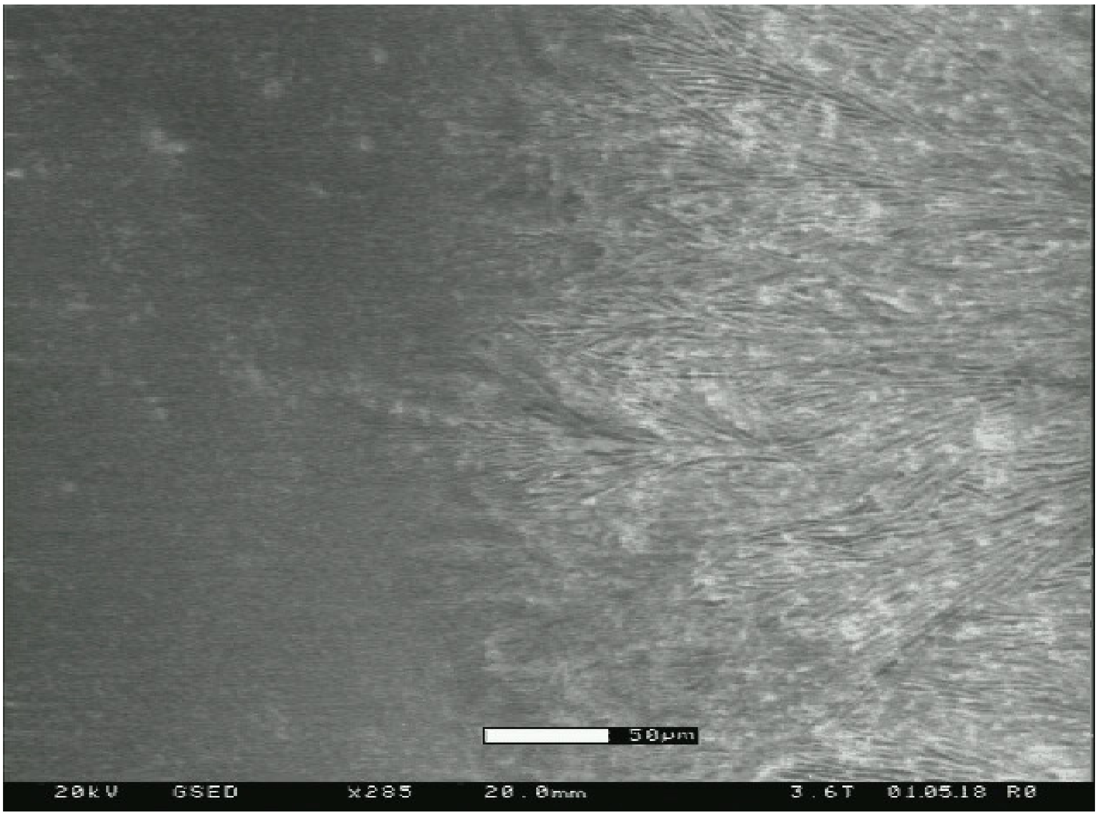

Figure 25. Rapid precipitation of mirabilite from solution in contact with fine-grained thenardite. Note crystals are growing from right to left. The left side is still largely solution and the right is largely crystals.

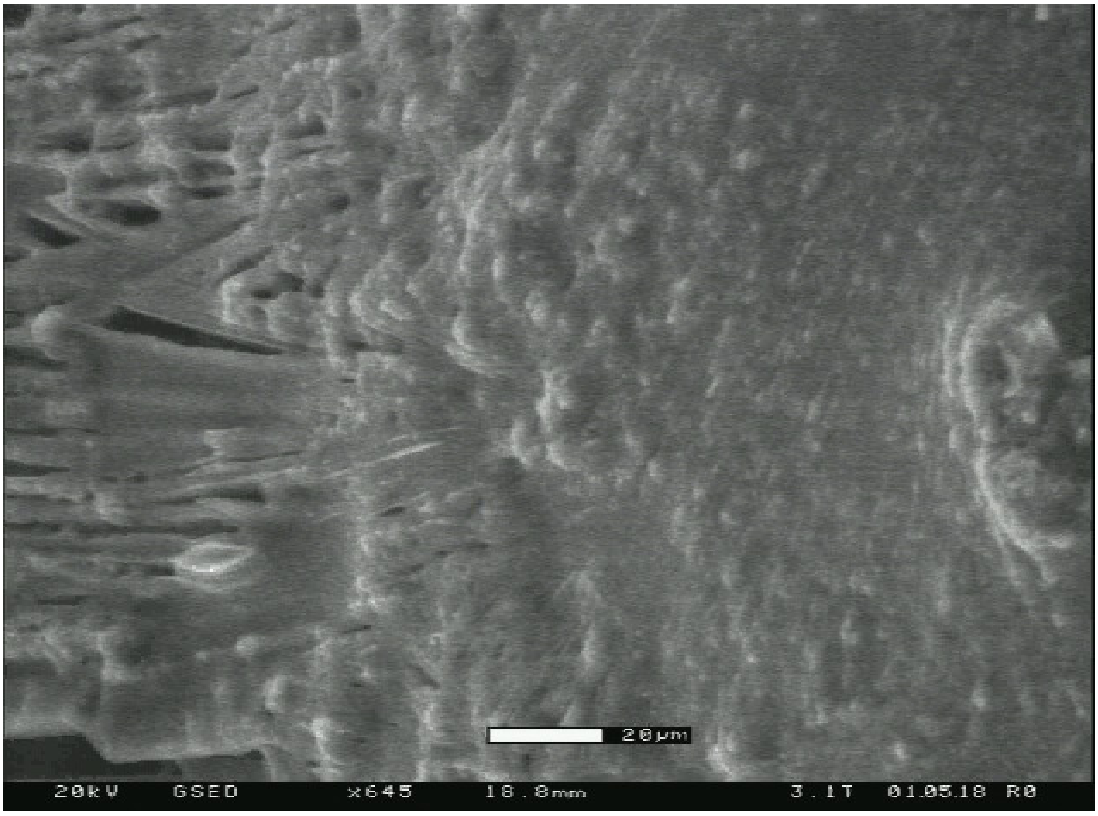

Figure 26. Rapid precipitation in ESEM of mirabilite from solution in contact with fine-grained thenardite. Note crystals grew from right to left. A water film is in the final stages of evaportion from the salt crystals.

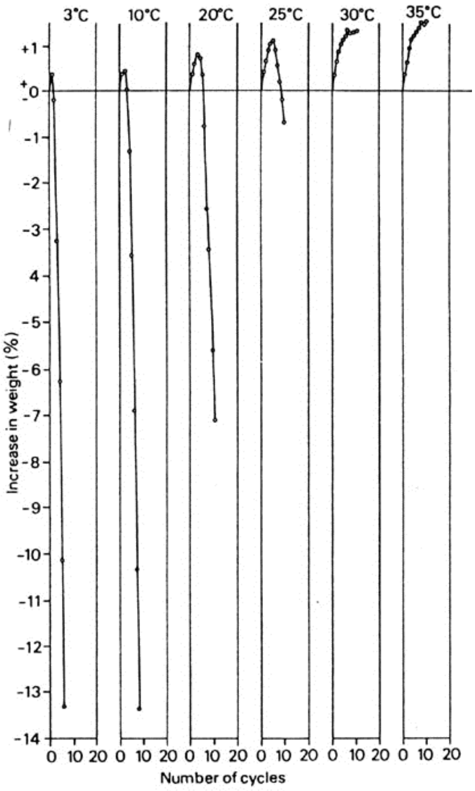

Figure 27. Influence of variation of soaking temperature of saturated salt soluion. Weight loss (gain) from standard salt crystallization test for stone (RILEM, ASTM). Diagram from Price (1978). Note much greater damage at lower temperatures.